

Adsorption of direct dye on palm ash: Kinetic and equilibrium modeling

A.A. Ahmad, B.H. Hameed*, N. Aziz

School of Chemical Engineering, Engineering Campus, University Science Malaysia, 14300 Nibong Tebal, Penang, Malaysia

Received 18 August 2005; received in revised form 21 June 2006; accepted 26 June 2006

Available online 28 June 2006

Abstract

Palm ash, an agriculture waste residue from palm-oil industry in Malaysia, was investigated as a replacement for the current expensive methods of removing direct blue 71 dye from an aqueous solution. The experimental data were analyzed by the Langmuir and Freundlich models of adsorption. Equilibrium data fitted well with Freundlich model in the range of 50–600 mg/L. The equilibrium adsorption capacity of the palm ash was determined with the Langmuir equation and found to be 400.01 mg dye per gram adsorbent at 30 °C. The rates of adsorption were found to conform to the pseudo-second-order kinetics with good correlation. The results indicate that the palm ash could be employed as a low-cost alternative to commercial activated carbon.

© 2006 Elsevier B.V. All rights reserved.

Keywords: Isotherm; Direct blue dye; Palm ash; Kinetics

1. Introduction

Textile wastewater is generally high in both color and organic content. Effluents discharged from dyeing industries are highly colored and they can be toxic to aquatic life in receiving waters [1,2]. Color removal from textile effluents has been given much attention in the last few years, not only because of its potential toxicity, but mainly due to its visibility problems [3,4]. The total dye consumption of the textile industry worldwide is in excess of 10⁷ kg/year, and an estimated 90% of this ends up on fabrics. Consequently, 1000 tonnes/year or more of dyes are discharged into waste streams by the textile industry worldwide [5].

Among several chemical and physical methods, the adsorption onto activated carbon has been found to be superior to other techniques in water-re-use methodology because of its capability for adsorbing a broad range of different types of adsorbates efficiently, and simplicity of design. However, commercially available activated carbons are still considered expensive [6]. Thus, many researchers researched for cheaper substitutes, which are relatively inexpensive, and are at the same time endowed with reasonable adsorptive capacity. These studies include the use of

coal [7], fly ash [8], activated clay [9], palm-fruit bunch [10], Bagasse pith [11], cellulose-based waste [12], peat, bentonite, slag and fly ash [13], rice husk [14], activated sludge [15], etc.

Solid waste from the palm-oil industry is highly abundant in Malaysia, which is one of the largest palm-oil exporters in the world. This waste is usually used as fuel in palm-oil mill factories. Then, after the combustion of oil-palm fibers and shell (used as boiler fuel for the steam generation in palm-oil mills) ash is produced. Malaysia thus generates huge loads of palm ash each year. Hence, the utilization of such agriculture solid waste residues for wastewater treatment is most desirable, first, as wastes are available abundantly at no or very low cost; second, as the disposal of these wastes normally poses a serious environmental problem in Malaysia, which has extensive agricultural activities. Therefore, the objective of this work is to study the utilization of palm ash as adsorbent to remove direct blue 71 dye from an aqueous solution. The equilibrium and kinetic studies have been performed.

2. Materials and methods

2.1. Adsorbent: palm ash

The palm ash was provided by United Oil Palm Mill, Penang, Malaysia. It was washed doubly with water and oven dried at

* Corresponding author. Tel.: +604 599 6422; fax: +604 594 1013.

E-mail address: chbassim@eng.usm.my (B.H. Hameed).

Nomenclature

b	adsorption energy constant of Langmuir adsorption isotherm (L/mg)
C_e	equilibrium liquid phase concentration (mg/L)
C_0	initial liquid phase concentration (mg/L)
k_1	rate constant of pseudo-first-order adsorption (1/min)
k_2	rate constant of pseudo-second-order adsorption (g/g min)
K_F	Freundlich isotherm constant related to adsorption capacity ((mg/g)(L/mg) ^{1/n})
n	Freundlich isotherm constant related to adsorption intensity
q_e	equilibrium solid phase adsorbate concentration (mg/g)
q_t	amount of adsorption at time t (mg/g)
Q	the maximum surface coverage (formation of monolayer) of sorbent (mg/g)
R_L	dimensionless separation factor
R^2	correlation coefficient
V	volume of solution (L)
W	mass of adsorbent (g)

110 °C overnight and sieved through sieve no. 100 (150 μm). Forty grams of palm ash are activated by refluxing with 250 mL of 40 wt.% H₂SO₄ at 340 K for 4 h in a round-bottom flask. The slurry was cooled in air and filtered through a glass fiber. The filter cake was repeatedly washed with hot deionized water until the filtrate was neutral.

2.2. Adsorbate: direct blue dye

Direct blue 71 dye, with the molecular formula C₄₀H₂₈N₇NaO₁₃S₄ (molecular weight 965.94) with CI No. 34140, was chosen as adsorbate. The dye was supplied by Sigma–Aldrich (M) Sdn Bhd, Malaysia. The chemical structure of the dye is shown in Appendix A.

2.3. Characterization of adsorbent

Adsorption of N₂ at 77 K was performed to evaluate the adsorptive properties of the palm ash. The value of BET surface area is obtained from the adsorption of N₂ at 77 K using Autosorb I, supplied by Quantachrome Corporation, USA. The BET specific surface area and average pore diameter of palm ash were found to be 5.356 m²/g and 2.263 nm, respectively.

The chemical composition of palm ash was determined using Rigaku RIX 3000 X-ray Fluorescence (XRF) spectrometer. It was found to have the composition: SiO₂ 40%, K₂O 12.1%, CaO 10.0%, Al₂O₃ 6.1%, MgO 6.4%, P₂O₅ 8.32%, C 5.4%, others 4.38% and its ignition loss was found to be 7.3%. The high oxide contents in palm ash give its structure the credibility as a good adsorbent.

2.4. Batch equilibrium studies

Adsorption isotherms were performed in a set of 43 Erlenmeyer flasks (250 mL), where solutions of dye (200 mL) with different initial concentrations (50–600 mg/L) were placed. An equal mass of 0.3 g of particle size (150 μm) palm ash was added to dye solutions, and the mixture was then kept in an isothermal shaker (30, 40 or 50 °C ± 1) for 4 h to reach equilibrium as a solid-solution mixture. A similar procedure was followed for another set of Erlenmeyer flask containing the same dye concentration without palm ash to be used as a blank. The pH was adjusted to 7 by adding either a few drops of diluted hydrochloric acid or sodium hydroxide. The flasks were then removed from the shaker; the final concentration of dye in the solution was measured at 594 nm using UV–vis spectrophotometer (Shimadzu UV/Vis 1601 Spectrophotometer, Japan). Each experiment was duplicated under identical conditions. The amount of adsorption at time t , q_t (mg/g), was calculated by

$$q_t = \frac{(C_0 - C_t)V}{W} \quad (1)$$

where C_0 and C_t (mg/L) are the liquid-phase concentrations of dye at initial and any time t , respectively, V the volume of the solution (L), and W is the mass of dry adsorbent used (g).

2.5. Batch kinetic studies

The procedures of kinetic experiments were basically identical to those of equilibrium tests. The aqueous samples were taken at present time intervals, and the concentrations of dye were similarly measured.

3. Results and discussion

3.1. Effect of agitation time and concentration of dye on adsorption

The effects of agitation time and dye concentration upon the removal of direct blue dye by palm ash at 30 °C are presented in Fig. 1. The amount adsorbed (mg/g) increased with the increase in agitation time and concentration, and remained nearly constant after equilibrium time. An increase in the initial dye concentration leads to an increase in the adsorption capacity of the dye on palm ash. The initial concentration provides an important driving force to overcome all mass transfer resistances of the dye between the aqueous solution and solid phases. Hence a higher initial concentration of dye enhances the sorption process. Fig. 1 also shows that most of the dye is adsorbed to achieve adsorption equilibrium in about 1 h, although the data were measured for 4 h. The time required to attain this state of equilibrium is termed equilibrium time, and the amount of dye adsorbed at the equilibrium time reflects the maximum adsorption capacity of the adsorbent under those operation conditions.

The adsorption capacity at equilibrium increases from 32 to 321 mg/g, with an increase in the initial dye concentration from 50 to 600 mg/L. At the beginning, the dye ions were adsorbed by the exterior surface of palm ash, so the adsorption rate was fast.

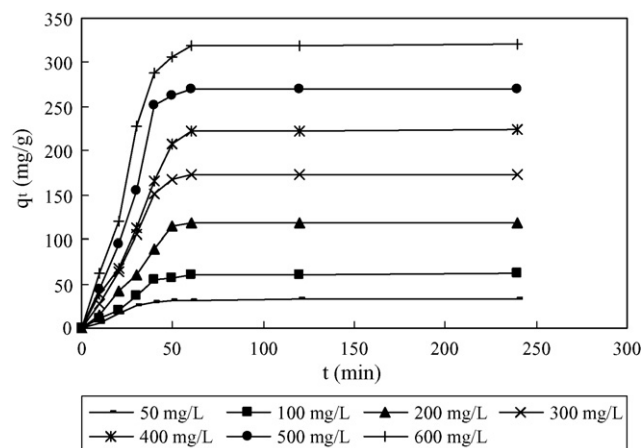


Fig. 1. The variation of adsorption capacity with adsorption time at various initial dye concentrations at 30°C.

When the adsorption of the exterior surface reached saturation, the dye ions entered into the pores of the palm ash particles and were adsorbed by the interior surface of the particle. This phenomenon takes relatively long contact time. The time profile of dye uptake is a single, smooth and continuous curve leading to saturation, suggesting also the possible monolayer coverage of dye on the surface of the palm ash. A similar phenomenon was observed for the adsorption of reactive blue 114, reactive yellow 64 and reactive red 124 dyes from an aqueous solution on calcined alunite and the equilibrium time was 2 h [16].

3.2. Adsorption isotherms

The relationship between the amount of a substance adsorbed at constant temperature and its concentration in the equilibrium solution is called the adsorption isotherm. Fig. 2 shows the adsorption isotherm of the direct blue dye at 30, 40 and 50°C. It is clear that the adsorption capacity at higher temperature is higher than that of lower temperature. The removal of direct blue dye by adsorption onto palm ash increased from 400.01 to 434.71 mg/g by increasing the temperature of the solution from 30 to 50°C (Table 1), indicating that the process is endothermic.

The equilibrium adsorption density q_e increases with the increase in dye concentration. Several models have been published in the literature to describe experimental data of adsorption isotherms. The Langmuir and Freundlich are the most frequently employed models. In this work, both models were used to describe the relationship between the amount of dye adsorbed and its equilibrium concentration.

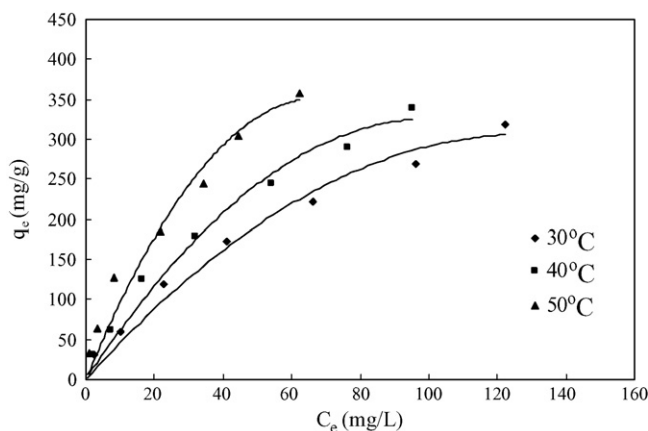


Fig. 2. Equilibrium adsorption isotherm of direct blue 71 dye on palm ash at different temperatures.

3.2.1. Langmuir isotherm

The following relation can represent the linear form of the Langmuir isotherm model:

$$\frac{1}{q_e} = \frac{1}{Q} + \frac{1}{bQ} \frac{1}{C_e} \quad (2)$$

where q_e is the amount adsorbed at equilibrium (mg/g), C_e the equilibrium concentration of the adsorbate (mg/L), and Q (mg/g) and b (L/mg) are the Langmuir constants related to the maximum adsorption capacity and the energy of adsorption, respectively. These constants can be evaluated from the intercept and the slope of the linear plot of experimental data of $1/q_e$ versus $1/C_e$ (Fig. 3a). Conformation of the experimental data into Langmuir isotherm model indicates the homogeneous nature of palm ash surface, i.e., each dye molecule/palm ash adsorption has equal adsorption activation energy. The results also demonstrate the formation of monolayer coverage of dye molecules on the outer surface of palm ash. Similar observations were reported for the adsorption of acid dyes (Acid Green 25, Acid Orange 10, Acid Red 18, Acid Red 73) on chitosan [17], and also for the adsorption of methylene blue on adsorbents materials produced from sewage sludge [18]. Values of Q and b were calculated from the intercept and slope of the linear plot and presented in Table 1. As seen in Table 1, the maximum adsorption capacities for direct blue dye onto palm ash at 30, 40, and 50°C were found to be 400.01, 416.66, and 434.71 mg/g, respectively. Maximum adsorption capacities of palm ash increased with increasing temperature.

The essential characteristics of the Langmuir equation can be expressed in terms of a dimensionless separation factor, R_L ,

Table 1
Langmuir and Freundlich parameters for adsorption of direct blue 71 dye on palm oil at different temperatures

Temperature (°C)	Langmuir isotherm model			Freundlich isotherm model		
	Q (mg g ⁻¹)	b (L/mg)	R^2	K_F ((mg/g)(L/mg) ^{1/n})	n	R^2
30	400.01	0.023	0.93	21.61	1.79	0.99
40	416.66	0.23	0.88	23.61	1.68	0.96
50	434.71	0.50	0.91	33.43	1.74	0.99

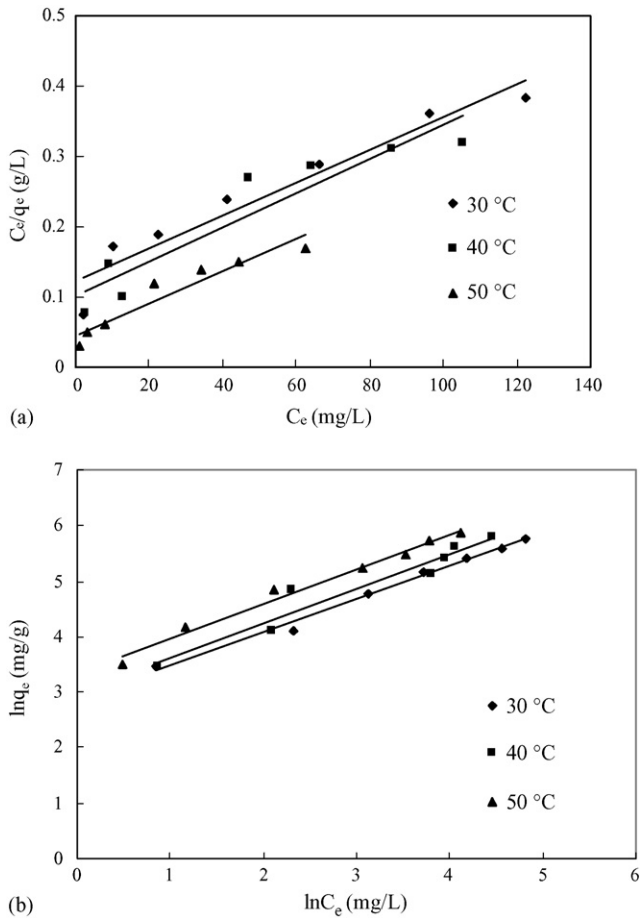


Fig. 3. (a) Linearized Langmuir isotherm for dye adsorption by palm ash at different temperatures; (b) linearized Freundlich isotherm for dye adsorption by palm ash at different temperatures.

defined [19] as

$$R_L = \frac{1}{1 + bC_0} \tag{3}$$

where C_0 is the highest initial solute concentration, b the Langmuir’s adsorption constant (L/mg). The R_L value implies the adsorption to be unfavorable ($R_L > 1$), linear ($R_L = 1$), favorable ($0 < R_L < 1$), or irreversible ($R_L = 0$). R_L values for direct dye adsorption onto palm ash were less than 1 and greater than zero indicating favorable adsorption under conditions used in this study.

3.2.2. Freundlich isotherm

The linear form of the Freundlich isotherm model is given by the following equation:

$$\ln q_e = \ln K_F + \frac{1}{n} \ln C_e \tag{4}$$

where K_F (mg/g)(L/mg)^{1/n} and $1/n$ are Freundlich constants related to adsorption capacity and adsorption intensity of the sorbent, respectively. Linear plot of $\ln q_e$ versus $\ln C_e$ shows that the adsorption of direct blue dye from an aqueous solution on palm ash also follows the Freundlich isotherm (Fig. 3b). Similar observations were reported for the adsorption of Direct Red 12B dye on biogas residual slurry [20], and also for the adsorption of methylene blue on adsorbent materials produced from sewage sludge [18]. Values of K_F and n are calculated from the intercept and slope, respectively, and are listed in Table 1. The value K_F of palm ash for direct blue dye at 30, 40, and 50 °C are on the order 21.61, 23.61, and 33.43, respectively. It is shown that n value is $1 < n < 2$, suggesting that the direct blue dye adsorption on palm ash is favorable [21]. Values of the correlation coefficient (R^2)

Table 2
Comparison of the maximum monolayer capacities of some dyes on various adsorbents

Dyes	Adsorbent	Langmuir isotherm		Freundlich isotherm		Reference
		Maximum monolayer adsorption capacities, Q^0 (mg/g)	b (L/mg)	K_F	n	
Direct blue 71	Palm ash	400.01	0.023	21.61	1.79	This work
Reactive blue 114	Calcined alunite	170.7	0.050	13.72	1.742	[16]
Reactive yellow 64	Calcined alunite	236	0.017	6.28	1.373	[16]
Reactive red 124	Calcined alunite	153	0.084	19.23	1.995	[16]
Acid brilliant blue	Banana pith	4.3	0.13	1	2.63	[27]
Acid violet	Coir pith	1.6	0.746	2.87	2.35	[28]
Acid brilliant blue	Coir pith	16.6	0.03	0.47	0.42	[28]
Rhodamine B	Coir pith	203.2	0.03	23.16	2.17	[28]
Acid blue 29	Peat	13.95	0.178	3.69	2.841	[13]
Acid blue 29	Fly ash	15.17	1.862	1.361	1.09	[13]
Basic blue 9	Bentonite	46.30	36.0	43.65	6.30	[13]
Basic blue 9	Fly ash	54.05	0.007	0.431	1.09	[13]
Dispersed red 1	Peat	49.73	0.094	5.18	1.71	[13]
Dispersed red 1	Bentonite	22.73	8.445	37.72	1.49	[13]
Dispersed red 1	Fly ash	30.03	0.106	3.71	1.77	[13]
Dispersed red 1	Slag	33.22	0.094	5.13	2.25	[13]
Methylene blue	Anaerobically sewage sludge (U_d)	114.943	0.0300	7.518	2.096	[18]
Methylene blue	Sewage sludge from agrofood industrial wastewater (A_d)	86.957	0.0076	2.434	1.856	[18]

(see Table 1) indicate that Freundlich isotherm has been best fitted for the adsorption of direct blue dye on palm ash.

Table 2 lists and compares the maximum monolayer adsorption capacity of some dyes on various adsorbents. Compared with some data in the literature, Table 2 shows that the palm ash studied in this work has a large adsorption capacity.

3.3. Adsorption kinetics

Kinetic adsorption data were treated with pseudo-first-order kinetic model [22]:

$$\frac{dq_t}{dt} = k_1(q_e - q_t) \tag{5}$$

where q_e and q_t refer to the amount of dye adsorbed (mg/g) at equilibrium and at any time, t (min), respectively, and k_1 is the equilibrium rate constant of pseudo-first-order sorption (1/min). Integration of Eq. (5) for the boundary conditions $t=0$ to t and $q_t=0$ to q_t , gives:

$$\log \frac{q_e}{q_e - q_t} = \frac{k_1}{2.303} t \tag{6}$$

which is the integrated rate law for a pseudo-first-order reaction. Eq. (6) can be rearranged to obtain a linear form:

$$\log(q_e - q_t) = \log q_e - \frac{k_1}{2.303} t \tag{7}$$

The slope and intercept of plot of $\log(q_e - q_t)$ versus t were used to determine the pseudo-first-order rate constant k_1 at 30 °C (Fig. 4). In many cases, the first order equation of Lagergren does not fit well with the whole range of contact time and is generally applicable over the initial stage of the adsorption processes [23].

Kinetic data were further treated with the pseudo-second-order kinetic model [24]. The differential equation is the following:

$$\frac{dq_t}{dt} = k_2(q_e - q_t)^2 \tag{8}$$

where k_2 is the equilibrium rate constant of pseudo-second-order adsorption (g/mg min). Integrating Eq. (8) for the boundary condition $t=0$ to t and $q_t=0$ to q_t , gives:

$$\frac{1}{q_e - q_t} = \frac{1}{q_e} + k_2 t \tag{9}$$

Table 3
Pseudo-first-order and pseudo-second-order adsorption rate constants and the calculated and experimental q_e values for adsorption of direct blue dye on palm ash at 30 °C

C_0 (mg/L)	$q_{e,exp}$ (mg/g)	Pseudo-first-order kinetic model			Pseudo-second-order kinetic model		
		$q_{e,cal}$ (mg/g)	k_1 (1/min)	R^2	$q_{e,cal}$ (mg/g)	k_2 (g/g min) $\times 10^{-2}$	R^2
50	32.17	21.60	21.71	0.81	35.84	0.140	0.96
100	61.10	40.08	26.31	0.65	70.42	0.052	0.96
200	119.25	147.67	18.55	0.81	147.05	0.017	0.90
300	173.62	173.30	18.79	0.79	204.08	0.017	0.94
400	223.81	284.44	18.96	0.79	270.27	0.015	0.94
500	270.68	416.38	14.28	0.91	322.58	0.013	0.93
600	321.17	289.50	19.64	0.82	357.14	0.012	0.95

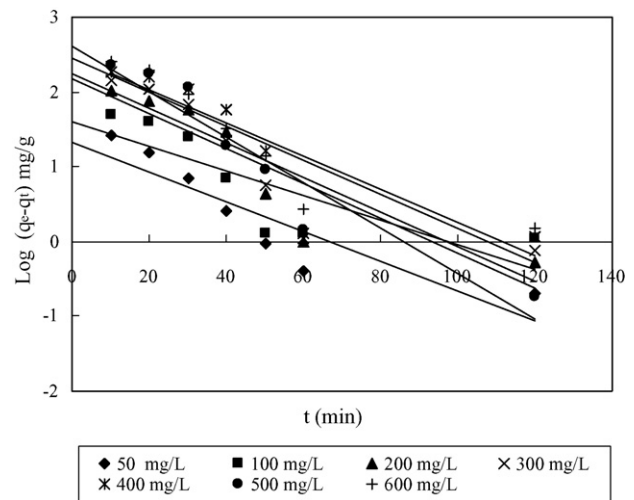


Fig. 4. Pseudo-first-order kinetics for adsorption of direct blue dye on palm ash at 30 °C.

which is the integrated rate law for a pseudo-second-order reaction. Eq. (9) can be rearranged to obtain a linear form:

$$\frac{t}{q_t} = \frac{1}{k_2 q_e^2} + \frac{1}{q_e} t \tag{10}$$

The slope and intercept of plot of t/q_t versus t were used to calculate the second-order rate constant k_2 at 30 °C (Fig. 5). It

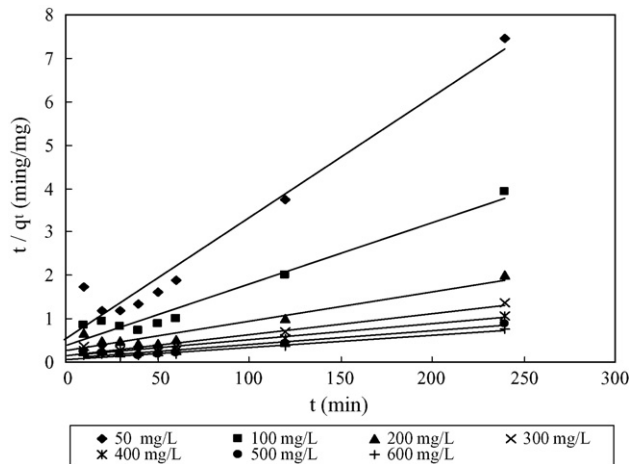


Fig. 5. Pseudo-second-order kinetics for adsorption of direct blue dye on palm ash at 30 °C.

is more likely to predict the behavior over the whole range of adsorption and is in agreement with the chemisorption mechanism being the rate-controlling step [23,24].

Table 3 lists the results of the rate constant studies for different initial dye concentrations by the pseudo-first-order and pseudo-second-order models at 30 °C. The correlation coefficient R^2 for the pseudo-second-order adsorption model has high value (>0.90); its calculated equilibrium adsorption capacity $q_{e,cal}$ is consistent with experimental data. These facts suggest that the pseudo-second-order adsorption mechanism is predominant, and that the overall rate of the dye adsorption process appears to be controlled by the chemisorption process [23,24]. Similar phenomena have also been observed in the biosorption of remazol black B on biomass [25], and in the adsorption of Methylene blue dyes on perlite [26]. For the second pseudo-order model in Table 3, the rate constant generally decreased with the increase of the initial dye concentration.

The benefit of using palm ash is two-fold since the problems associated with management of the waste are also ameliorated. Recovery and regeneration of some adsorbents is difficult, whereas the palm ash as adsorbent could be disposed of safely by burning after drying.

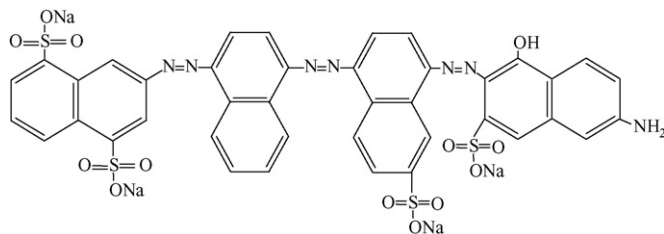
4. Conclusion

Palm ash was used as an adsorbent for the removal of direct blue 71 dye from an aqueous solution. The palm ash had very high adsorption capacity to remove the dye, with a maximum monolayer adsorption capacity was 400.01 mg/g at 30 °C. The adsorption capacities were affected by the initial dye concentration. The uptake increased with the increase in initial dye concentration. The Freundlich equation agrees very well with the equilibrium isotherm. The pseudo-second-order kinetic model fits very well with the dynamical adsorption behavior of direct blue dye. This agriculture waste residue could therefore substituted be in place of activated carbon as adsorbent due to its availability, high adsorption capacity and low cost.

Acknowledgment

The authors acknowledge the research grant provided by University Science Malaysia, Penang, Malaysia that has resulted in this article.

Appendix A. Chemical structure of direct blue 71 dye



References

- [1] C.K. Lee, K.S. Low, P.Y. Gan, Removal of some organic dyes by acid treated spent bleaching earth, *Environ. Technol.* 20 (1999) 99–104.
- [2] K. Kadirvelu, M. Kavipriya, C. Karthika, M. Radhika, N. Vennilamani, S. Pattabhi, Utilization of various agriculture wastes for activated carbon preparation and application for the aqueous solutions, *Bioresource Technol.* 87 (2003) 129–132.
- [3] R.Y.-L. Yeh, A. Thomas, Color difference measurement and color removal from dye wastewaters using different adsorbents, *J. Chem. Technol. Biotechnol.* 63 (1995) 55–59.
- [4] L.C. Morais, O.M. Freitas, E.P. Gancelves, L.T. Vaskancelos, C.G. Gonzalez Beca, Reactive dyes removal from wastewaters by adsorption on eucalyptus bark: variables that define the process, *Water Res.* 33 (1999) 979–988.
- [5] R. Marc, Asian textile dye makers are a growing power in changing market, *C EN Northeast News Bureau* 73 (1996) 10–12.
- [6] S. Chakraborty, S. De, S. DasGupta, J.K. Basu, Adsorption study for the removal of basic dye: experimental and modeling, *Chemosphere* 58 (2005) 1079–1086.
- [7] S. Venkata Mohan, N. Chandrasekhar Rao, J. Karthikeyan, Adsorption removal of direct azo dye from aqueous phase onto coal based sorbents: a kinetic and mechanistic study, *J. Hazard. Mater.* 90 (2002) 189–204.
- [8] D. Mohan, K.P. Singh, G. Singh, K. Kumar, Removal of dyes from wastewater using fly ash, a low-cost adsorbent, *Ind. Eng. Chem. Res.* 41 (2002) 3688–3695.
- [9] F.-C. Wu, R.-L. Tseng, R.-S. Juang, Kinetics of color removal by adsorption from water using activated clay, *Environ. Technol.* 22 (2001) 721–729.
- [10] M.M. Nassar, The kinetics of basic dye removal using palm-fruit bunch, *Adsorp. Sci. Technol.* 15 (1997) 609–617.
- [11] G. McKay, Application of surface diffusion model to the adsorption of dyes on bagasse pith, *Adsorption* 4 (1998) 361–372.
- [12] G. Annadurai, R.-S. Juang, D.-J. Lee, Use of cellulose-based wastes for adsorption of dyes from aqueous solutions, *J. Hazard. Mater.* B92 (2002) 263–274.
- [13] K.R. Ramakrishna, T. Viraraghavan, Dye removal using low cost adsorbents, *Water Sci. Technol.* 36 (1997) 189–196.
- [14] K.S. Low, C.K. Lee, Quaternized rice husk as sorbent for reactive dyes, *Bioresource Technol.* 61 (1997) 121–125.
- [15] Z. Aksu, Biosorption of reactive dyes by dried activated sludge: equilibrium and kinetic modeling, *Biochem. Eng. J.* 7 (2001) 79–84.
- [16] M. Özacar, İ.A. Sengil, Adsorption of reactive dyes on calcined alunite from aqueous solution, *J. Hazard. Mater.* B 98 (2003) 211–224.
- [17] Y.C. Wong, Y.S. Szeto, W.H. Cheung, G. McKay, Adsorption of acid dyes on chitosan-equilibrium isotherm analyses, *Process Biochem.* 39 (2004) 693–702.
- [18] M. Otero, F. Rozada, L.F. Calvo, A.I. Garcia, A. Moran, Kinetic and equilibrium modelling of the methylene blue removal from solution by adsorbent materials produced from sewage sludges, *Biochem. Eng. J.* 15 (2003) 59–68.
- [19] G. McKay, H.S. Blair, J.R. Gardner, The adsorption of dyes onto chitin in fixed bed columns and batch adsorbers, *J. Appl. Polym. Sci.* 29 (1984) 1499–1514.
- [20] C. Namasivayam, R.T. Yamuna, Adsorption of direct red 12B by biogas residual slurry: equilibrium and rate processes, *Environ. Pollut.* 89 (1995) 1–7.
- [21] K. Kadirvelu, K. Thamaraiselvi, C. Namasivayam, Adsorption of nickel(II) from aqueous solution onto activated carbon prepared from coirpith, *Sep. Purif. Technol.* 24 (2001) 497–505.
- [22] S. Lagergren, Zur theorie der sogenannten adsorption gelöster stoffe, *K. Sven. Vetenskapsakad. Handl.* 24 (1898) 1–39.
- [23] G. McKay, Y.S. Ho, The sorption of lead(II) on peat, *Water Res.* 33 (1999) 578–584.
- [24] G. McKay, Y.S. Ho, Pseudo-second order model for sorption processes, *Process Biochem.* 34 (1999) 451–465.
- [25] Z. Aksu, S. Tezer, Equilibrium and kinetic modelling of biosorption of Remazol Black B by *Rhizopus arrhizus* in a batch system: effect of temperature, *Process Biochem.* 36 (2000) 431–439.

- [26] M. Doğan, M. Alkan, A. Türkyilmaz, Y. Özdemir, Kinetics and mechanism of removal of methylene blue by adsorption onto perlite, *J. Hazard. Mater.* 109 (2004) 141–148.
- [27] C. Namasivayam, D. Prabha, M. Kumutha, Removal of direct red and acid brilliant blue by adsorption on to banana pith, *Bioresource Technol.* 64 (1998) 77–79.
- [28] C. Namasivayam, M.D. Kumar, K. Selvi, R.A. Begum, T. Vanathi, R.T. Yamuna, 'Waste' coir pith—a potential biomass for the treatment of dyeing wastewaters, *Biomass Bioenergy* 21 (2001) 477–483.